THE COMPANY OF
Biologists

RESEARCH ARTICLE

Glycolysis plays an important role in energy transfer from the base to the distal end of the flagellum in mouse sperm

Gen L. Takei*, Daisuke Miyashiro, Chinatsu Mukai‡ and Makoto Okuno§,¶

ABSTRACT

Many studies have been conducted to elucidate the relationship between energy metabolic pathways (glycolysis and respiration) and flagellar motility in mammalian sperm, but the contribution of glycolysis to sperm motility has not yet been fully elucidated. In the present study, we performed detailed analysis of mouse sperm flagellar motility for further understanding of the contribution of glycolysis to mammalian sperm motility. Mouse sperm maintained vigorous motility in the presence of substrates either for glycolysis or for respiration. By contrast, inhibition of glycolysis by alpha-chlorohydrine caused a significant decrease in the bend angle of the flagellar bending wave, sliding velocity of outer doublet microtubules and ATP content even in the presence of respiratory substrates (pyruvate or β-hydroxybutyrate). The decrease of flagellar bend angle and sliding velocity are prominent in the distal part of the flagellum, indicating that glycolysis inhibition caused the decrease in ATP concentration thererin. These results suggest that glycolysis potentially acts as a spatial ATP buffering system, transferring energy (ATP) synthesized by respiration at the mitochondria located in the basal part of the flagellum to the distal part. In order to validate that glycolytic enzymes can transfer high energy phosphoryls, we calculated intraflagellar concentration profiles of adenine nucleotides along the flagellum by computer simulation analysis. The result demonstrated the involvement of glycolysis for maintaining the ATP concentration at the tip of the flagellum. It is likely that glycolysis plays a key role in energy homeostasis in mouse sperm not only through ATP production but also through energy transfer.

KEY WORDS: Mammalian sperm, Motility, Glycolysis, Energy transport, Metabolism, Flagellar bending

INTRODUCTION

Mammalian sperm flagella require motility for a long period of time from ejaculation to accomplish fertilization (Austin, 1985). For the maintenance of motility during such a long period, mammalian sperm must continue to metabolize extracellular energy substrates to produce ATP. Therefore, elucidation of the correlation between flagellar movement and energy metabolism is very important to understand the functional features of the mammalian sperm. Furthermore, it has been expected to be applied to the treatment of male infertility and contraceptive technologies.

Department of Life Sciences, Graduate School of Arts and Sciences, The University of Tokyo Komaba 3-8-1, Meguro-ku, Tokyo, 153-8902 Japan. *Present address: Cardiovascular Physiology, Okayama University Graduate School of Medicine, Dentistry and Pharmaceutical Science 2-5-1, Shikada-cho, Kita-ku, Okayama-city, Okayama 700-8558 Japan. ‡Present address: Baker Institute for Animal Health, College of Veterinary Medicine, Cornell University, Ithaca, NY 14853, USA. §Present address: Department of Biosciences, Chuo University 1-13-27 Kasuga, Bunkyo-ku, Tokyo 112-8551 Japan.

¶Author for correspondence (macokuno@gmail.com)

There are two major metabolic pathways to produce ATP, glycolysis and respiration. Most mammalian sperm must produce ATP to maintain vigorous motility by one or both of the pathways, which are localized in different regions of the sperm. Mitochondria that perform respiration are localized in the mid-piece, the basal limited locus of flagellum. However, glycolysis works in the principal piece of flagella occupying major part of flagellum, as several glycolytic enzymes have been reported to be localized on the fibrous sheath, a cytoskeletal structure that goes through the entire length of the sperm tail (Krisfalusi et al., 2006; Westhoff and Kamp, 1997). Because of the higher efficiency of ATP production and an abundance of mitochondria in mammalian sperm, respiration has been considered to be a major source of ATP production.

A recent study, however, demonstrated that glycolysis plays a major role in ATP production in mouse sperm flagellar movement (Mukai and Okuno, 2004). Glyceraldehyde-3-phosphate dehydrogenase (GAPDH), one of the glycolytic enzymes that catalyze glyceraldehyde-3-phosphate (GAP) to 1,3-bisphosphoglycerate (1,3BPG), is abundantly localized to the fibrous sheath in porcine, human, bovine, equine and murine sperm (Westhoff and Kamp, 1997; Welch et al., 2000). Genetic deletion of the sperm-specific isoenzyme of GAPDH, GAPDS, using a knock-out model gave rise to sperm immotility even in the presence of pyruvate, a respiration substrate, resulting in infertility (Miki et al., 2004). In addition to GAPDS, proteomic studies revealed that multiple glycolytic enzymes (hexokinase, aldolase, phosphoglycerate kinase, enolase, pyruvate kinase and lactate dehydrogenase) were demonstrated to localize in the fibrous sheath in mouse sperm (Krisfalusi et al., 2006). It was also reported that the knock-out mouse of sperm-specific glycolytic enzymes, lactate dehydrogenase C (LDHC) and phosphoglycerate kinase 2 (PGK2), resulted in infertility in mice (Odet et al., 2008; Danshina et al., 2010). These studies supported that glycolysis in the principal piece of the flagellum is a crucial ATP production pathway in mouse sperm.

Another serious problem that must be solved is how ATP synthesized in mitochondria at the base of the flagellum is supplied sufficiently to the distal end of the flagellum, because ATP is necessary at the end of the flagellum for active bending movement. In sea urchins, the problem is solved by the 'creatine shuttle', an energy transporting system from mitochondria at the base to the tip of the flagella (Tombes et al., 1987). However, such an energy transferring system has not been detected in mice, although mouse sperm have a longer flagellum (120 μm) than sea urchin sperm (40 μm) (Kamp et al., 1996). These results suggest that mitochondria-synthesized ATP is not assumed to be supplied to the tip of flagellum sufficiently. Based on these studies, it has been considered that ATP necessary for flagellar movement is produced mainly by glycolysis.

However, there are some contradicting reports (Ford, 2006; Tanaka et al., 2004). Tanaka and colleagues (Tanaka et al., 2004) reported that a testis-specific isoenzyme of succinyl CoA transferase

List of abbreviations

1,3-BPG	1,3-bisphosphoglycerate
3PG	3-phosphoglycerate
ACH	α-chlorohydrin
ADP	adenosine diphosphate
AK	adenylate kinase
AMP	adenosine monophosphate
ANP	adenine nucleotide phosphate
ATP	adenosine triphosphate
BHB	β-hydroxybutyrate
CE-TOFMS	capillary electrophoresis electrospray ionization time-of-flight mass spectrometry
DOG	2-deoxy-D-glucose
GAP	glyceraldehyde-3-phosphate
GAPDH	glyceraldehyde-3-phosphate dehydrogenase
GAPDS	glyceraldehyde-3-phosphate dehydrogenase, spermatogenic
Glc	glucose
HPLC	high performance liquid chromatography
PGK	phosphoglycerate kinase
P_i	inorganic phosphate
Pyr	pyruvate

(SCOT-t) is expressed in mouse sperm. SCOT-t is necessary to metabolize D-β-hydroxybutyrate (BHB), a substrate of respiration. When BHB was supplemented to the sperm suspension instead of glucose, the percentage of sperm motility was not affected by α-chlorohydrin (ACH), a potent inhibitor of GAPDH. Moreover, it was reported that intracellular ATP concentration was not decreased by ACH in the absence of glucose (Ford and Harrison, 1985; Ford and Harrison, 1986). These results support that respiration is enough to supply ATP for sperm motility.

As mentioned above, there are some contradictory results about the relationship between metabolic pathways and sperm motility. These studies were focused on which metabolic pathway (glycolysis or respiration) was important and dominant for sperm motility, and did not address the possibility that these two metabolic pathways may contribute to the flagellar movement differently. To investigate this possibility, a more detailed analysis of flagellar movement seems to be necessary.

In previous studies, flagellar movement was assessed by the percentage of motile sperm or the beat frequency of flagellum. However, these parameters were insufficient to evaluate the 'magnitude' of flagellar bending, an important parameter for evaluating the amount of microtubule sliding. Flagellar bending motion is produced through sliding of the pairs of doublet microtubules by forces produced by dynein arms that hydrolyze ATP. Therefore, microtubule sliding velocity, resulting from the rate of ATP hydrolysis, is directly related to ATP concentration, which is the result of consumption and production. In order to assess the contribution of ATP production pathways to flagellar movement,

sliding velocity was calculated as a product of beat frequency and bend angle. It was reported that sliding velocity correlates with ATP concentration (Yano and Miki-Noumura, 1980; Si and Okuno, 1995). Therefore, a change of sliding velocity could be assumed to directly reflect the change of ATP concentrations. Furthermore, the local bending along the flagellum is tightly coupled to the local sliding velocity because the beat frequency of the flagellum is constant throughout the entire length of the flagellum (Okuno and Hiramoto, 1976), and thus leads to an evaluation of local concentrations of ATP therein.

In the present study, the correlation between metabolic pathways, especially glycolysis, and flagellar movement was re-evaluated by detailed motility analysis (measurement of beat frequency, bend angle, sliding velocity and local bending). Our results suggest that glycolysis functions not only as an ATP production system, but also as an energy transferring system through spatial buffering of ATP.

RESULTS

Change of motility depends on metabolic substrate

First, differences of motility induced by substrates (glucose, pyruvate and BHB) were evaluated by detailed analysis of flagellar movement using various parameters (beat frequency, bend angle and sliding velocity of microtubules). Results are summarized in Table 1. Mouse sperm commonly exhibited high motility (<10 Hz beat frequency, <30 rad s^{-1} sliding velocity) at 10 mmol l^{-1} of each substrate, and very few differences in motility parameters (beat frequency, bend angle, percentage of motility, sliding velocity and waveform of flagella) were observed among the substrates.

Effect of glycolysis inhibition on flagellar movement

Sperm maintained vigorous motility for more than 60 min in the presence of glucose, pyruvate or BHB (Table 1). This result indicates that mouse sperm can produce sufficient ATP to sustain motility by either glycolysis or respiration alone. We then observed the effect of glycolysis inhibition on sperm motility to clarify the contribution of glycolysis on sperm motility. Fig. 1 shows changes in beat frequency, bend angle and sliding velocity with time in the presence or absence of α-chlorohydrin (ACH). When glycolysis was inhibited by ACH in the presence of glucose, mouse sperm stopped swimming by 60 min (Fig. 1). In contrast, the beat frequency of sperm was not affected by ACH for at least 60 min, when substrate for respiration, i.e. BHB or pyruvate, was added to the test solution (Fig. 1A) instead of glucose. However, the bend angle of flagella was significantly inhibited by ACH at 30 and 60 min after activation even in the presence of BHB or pyruvate (Fig. 1B). As a result, sliding velocity was significantly reduced by ACH to less than 30 rad s^{-1} at 30 and 60 min after activation (Fig. 1C). Similar results were obtained when glycolysis was inhibited by 2-deoxy-D-glucose (DOG), an analog of glucose that inhibits hexokinase (Hiipakka and

Table 1. Differences in beat frequency, bend angle, sliding velocity and waveform of sperm flagella depend on energy substrate

Parameter	Glucose (n=16)	Pyruvate (n=9)	β-hydroxy butyrate (n=17)
Beat frequency (Hz)	16.3±0.70	14.6±0.72	16.9±1.13
Bend angle (rad)	2.55±0.12	2.62±0.07	2.63±0.16
Sliding velocity (rad s^{-1})	41.0±1.91	38.1±1.60	42.6±2.26
Motility (%)	55.8±4.60	58.8±2.43	56.3±3.92
Waveform			

Data are means ± s.e.m. No significant difference in motility parameters was recognized. The concentration of substrates was 10 mmol l^{-1}.
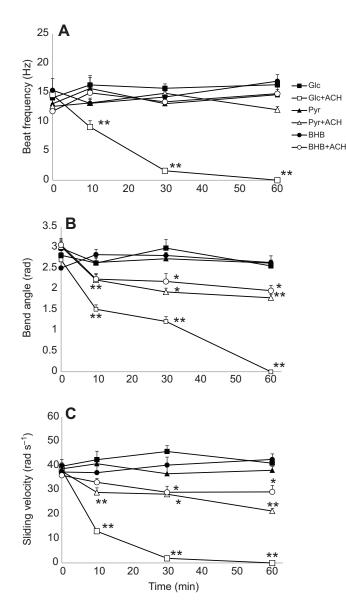
Fig. 1. Effect of α-chlorohydrin (ACH) on sperm flagellar motility in the presence of various substrates. Sperm was diluted into media containing substrates only or substrates and inhibitor. Then, change in beat frequency (A), bend angle (B) and shear angle (C) was plotted against time course. Both the shear angle and the bend angle are represented as the averaged absolute values obtained from both the principal and reverse bend. Beat frequency was not significantly reduced by ACH when pyruvate or β-hydroxy butyrate (BHB) was present in the media. By contrast, bend angles and shear angles were significantly reduced by ACH even when pyruvate or BHB was present in the media. Concentrations of substrates and inhibitor were 10 mmol l^{-1}. Error bars represent s.e.m. (N>9). Asterisks indicate a significant difference from control sperm (*P<0.05, **P<0.01). Glc, glucose; Pyr, pyruvate.

Hammerstedt, 1978; Hyne and Edwards, 1985) (data not shown). Because sliding velocity was known to correlate with ATP concentration (Yano and Miki-Noumura, 1980; Si and Okuno, 1995), these results indicated a decrease in intracellular ATP by ACH even in the presence of respiratory substrates.

Effect of glycolysis inhibition on local bending of flagellum
Glycolysis-inhibited sperm showed unchanged beat frequency and significantly reduced bend angle in the presence of respiratory substrates. To further characterize the decrease in bend angle, local bending along the flagellum was investigated in every 10 μm by measuring the shear angle.

In the presence of respiratory substrates and absence of ACH, local shear angle in the flagellum increased as the bending wave propagated to the distal end, except for a 'singular point' at 70 μm, where tangent line and reference line synchronously keep rather parallel (BHB or pyruvate; Fig. 2A,B). In contrast, sperm whose glycolysis was inhibited by ACH did not show such an increase along the flagellar axis in the shear angle. The shear angle of the flagellum was almost unchanged from the basal region to the distal end of the flagellum (Fig. 2A,B). Similar results were obtained with DOG. These results indicate that inhibition of glycolysis abolished the increase in the shear angle toward the distal end of the flagellum.

Data shown in Fig. 2A,B were re-plotted as the ratio of local bending by dividing shear angle in glycolysis-inhibited sperm by that in the control sperm (Fig. 2C,D). The ratio of local bending of glycolysis-inhibited sperm was high at the basal region of the flagellum (approximately 0.7), suggesting that the inhibition was low, but was considerably reduced at the tip of the flagellum (approximately 0.5).

In addition to the evaluation of local bending by the shear angle, local bending was evaluated by the bend angle in order to eliminate the 'singular point' observed in Fig. 2A,B (Fig. 3). Similar to the result of shear angle (Fig. 2A,B), sperm showed a gradual increase in bending as the wave propagated when glycolysis was not inhibited by ACH (filled symbols). By contrast, glycolysis-inhibited sperm (open symbols) did not show as a large an increase as those without ACH, consistent with the results of the shear angles (Fig. 2A,B). These results indicate that reduction of bending is prominent in the distal region of the flagellum.

Effect of glycolysis inhibition on the content of adenine nucleotide phosphate in sperm
Glycolysis-inhibited sperm showed decreased bend angles and sliding velocities despite the presence of respiratory substrates, suggesting a decrease in ATP concentration. In order to examine whether intracellular ATP was decreased, adenine nucleotide phosphate (ANP, including ATP, ADP and AMP) content was directly measured by reversed-phase high performance liquid chromatography (HPLC) in mouse sperm 30 min after activation. Fig. 4 shows the change in ANP content by the inhibition of glycolysis.

When glucose was added to the media as a metabolic substrate, a higher content of ATP (approximately 0.4 nmol 10^{-6} sperm) and lower contents of ADP and AMP (approximately 0.16 and 0.07 nmol 10^{-6} sperm, respectively) were measured than in sperm incubated in the absence of substrates. Similarly, high contents of ATP and low contents of ADP and AMP were observed in the presence of respiratory substrates (Pyr and BHB). There was no significant difference between them. ACH treatment, however, caused a drastic decrease in ATP content (P<0.01) and increase in AMP content (P<0.01) in the presence of glucose. ACH treatment also caused a decrease in ATP content and increase in ADP and AMP content in the presence of pyruvate and BHB. These results suggest that inhibition of glycolysis by ACH causes metabolic perturbation even in the presence of respiratory substrates.

Metabolome analysis
In order to determine the intracellular state of metabolic intermediates, metabolomic analysis by capillary electrophoresis electrospray ionization time-of-flight mass spectrometry (CE-TOFMS) was conducted (Table 2). Intracellular ATP content
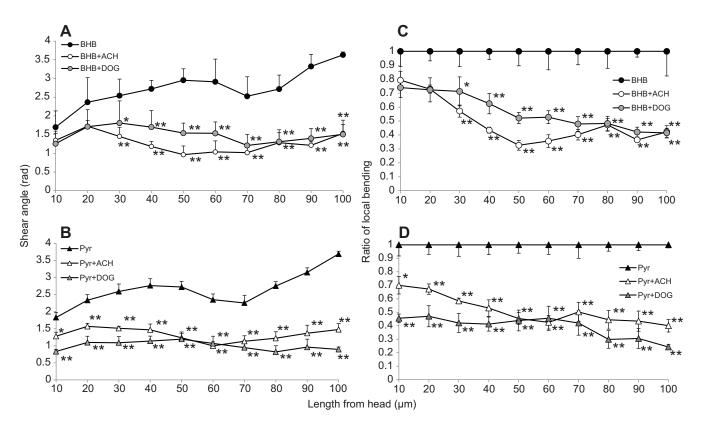
Fig. 2. Changes of local bending along the glycolysis-inhibited sperm flagella. Sperm were diluted into media containing respiration substrates (A: BHB; B: Pyr) and glycolysis inhibitor [ACH or 2-deoxy-D-glucose (DOG)], then allowed to swim in the media for 1 h in a CO_2 incubator (37°C, 5% CO_2, 95% air). After incubation, local shear angle was measured with the computer software Bohboh. Changes of shear angle are plotted at indicated distance from the head (A,B). Data shown in A and B were expressed as the ratio of the shear angle in the control to that in the glycolysis-inhibited sperm (C,D). Bending decreases in the distal part of flagellum. The concentration of each substrate and inhibitor was 10 mmol l^{-1}. Error bars represent s.e.m. N=5. Asterisks indicate a significant difference from control sperm (*P<0.05, **P<0.01).

determined by metabolomic analysis was 0.368 nmol 10^{-6} sperm. This value was approximately the same as that determined by HPLC (Fig. 4), indicating the accuracy of metabolomic analysis. Calculated concentrations of total intracellular ANP and total PGK substrates (total 3PG and 1,3BPG) were 11.6 and 0.155 mmol l^{-1}, respectively (Table 2). The cytosolic volume used to calculate the intracellular concentration of each parameter was 53.5 fl (Yeung et al., 2002). The values used for the following computer simulation are shown in Table 2.

Computer simulation

As described above, glycolysis inhibition caused a decrease in the sliding velocity at the distal part of the flagellum, indicating the deficiency of ATP therein in spite of the presence of respiratory substrates. These results suggest that ATP synthesized by mitochondria at the base (mid piece) could not be supplied to the distal part of the flagellum sufficiently when glycolysis is inhibited. This phenomenon raised the possibility that glycolysis functions as a spatial buffering of ATP along mouse sperm flagellum, transferring the 'energy wave' from the mid piece to the distal end.

In previous studies, it was reported that glycolytic enzymes, particularly phosphoglycerate kinase (PGK), have the potential to transfer energy in muscle cells through buffering of ATP (Dzeja et al., 2004; Dzeja and Terzic, 2003). To assess the possibility that glycolysis has the potential to transport energy to the distal end of the flagellum in mouse sperm, the concentrations of high energy phosphoryls (ATP and ADP) along the flagellum were calculated by simulating the intraflagellar diffusion of high energy phosphoryls *in*

silico. The algorithms of the simulation were based on the simulation model by Tombes et al. that verified the energy transfer potential of creatine kinase in sea urchin sperm (Tombes et al., 1987). The diffusing length of the flagellum was set to 100 µm although murine sperm has a 120 µm flagellum, because the mid piece, a mitochondria-rich region, is as long as 20 µm. Fig. 5 illustrates the results of calculations of ATP, ADP and ATPase activity profiles along the flagellum.

It was reported that adenylate kinase (AK) also participates in energy transfer (Dzeja and Terzic, 2003). Because AK is abundantly present throughout the mouse sperm flagella (Cao et al., 2006), the reaction of AK was also considered in the equation. The parameters of AK used in the simulation were obtained from data on rabbit muscle AK (Noda, 1973). When the reaction by AK is included and glycolysis (PGK) is excluded in the simulation, ATP at the tip of the flagellum decreased from 11.4 mmol l^{-1} (basal concentration) to 5.45 mmol l^{-1}, whereas ADP at the tip increased from 0.2 mmol l^{-1} (basal concentration) to 3.71 mmol l^{-1} (data not shown). The ratio of the total amount of intraflagellar ATP to the total ADP calculated by computer simulation was approximately 5:2 under this condition where only AK operates in ATP transfer. This ratio was quite different from the ratio of the total intracellular ATP to total intracellular ADP of glycolysis-inhibited sperm determined by HPLC analysis, which was approximately 5:4 (Fig. 4). When both AK rate and PGK rate were reduced to zero (in other words, when ATP at the distal region was assumed to be supplied only by simple diffusion from the mid piece without ATP buffering), the ratio of the total intraflagellar ATP to the total intraflagellar ADP was calculated
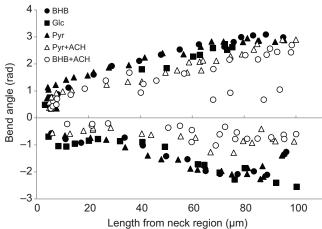
Fig. 3. Scattergram of typical changes of local bend angle with the length of flagella. Sperm were diluted into media containing respiration substrates and glycolysis inhibitor (ACH), then allowed to swim in the media for 1 h in a CO_2 incubator (37°C, 5% CO_2, 95% air). After incubation, local bend angle was determined for flagella of sperm attached to the glass surface by the head. Measurement was performed as described in the Materials and methods. ACH-treated sperm (open symbols) showed reduced bend angles compared with non-treated controls (filled symbols). The concentrations of each substrate and inhibitor were 10 mmol l^{-1}.
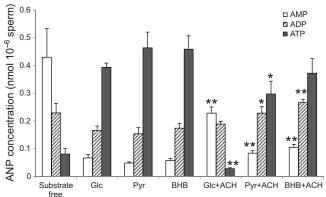

Fig. 4. Effect of glycolytic inhibitor on the content of adenine nucleotide phosphate (ANP) in sperm. Content of ANPs were measured by reversed-phase HPLC 30 min after activation. Decrease in the ATP content and increase in the ADP and AMP contents by ACH were observed even in the presence of respiratory substrates. The concentration of each substrate and inhibitor was 10 mmol l^{-1}. Data are means ± s.e.m. of 15 mice. Asterisks indicate a significant difference from control sperm (*$P<0.05$, **$P<0.01$).

to be approximately 5:4, similar to the ratio determined by HPLC in glycolysis-inhibited sperm (Fig. 5, red lines). These results suggest that AK activity may be so low that we can neglect its involvement in the energy transferring system in mouse sperm under physiological conditions despite the presence of AK (Cao et al., 2006). Therefore, in the following calculations, ANP profiles along the flagellum were made without AK activity (Fig. 5).

When PGK activity was reduced to zero, a drastic decrease was observed in ATP concentration, from 11.4 mmol l^{-1} (basal concentration) to 4.32 mmol l^{-1}, as well as an increase in ADP concentration, from 0.2 mmol l^{-1} (basal concentration) to 7.13 mmol l^{-1}, at the tip of flagellum. The resultant activity of dynein ATPase at the tip of the flagellum attenuated from 0.133 mmol l^{-1} s^{-1} (basal value, this value is constant among

calculations) to 0.0738 mmol l^{-1} s^{-1}. ATPase activity was calculated using Eqn 2 (see Materials and methods). This means that the ATPase rate at the tip of the flagellum decreased to approximately 55% of the basal value.

When the PGK reaction was included in the equation, a slight increase in ATP concentration from 4.32 to 4.5 mmol l^{-1} and a decrease in ADP concentration from 7.13 to 7.0 mmol l^{-1} were observed in the presence of 0.155 mmol l^{-1} PGK substrates (total 3PG and 1,3BPG). The resultant ATPase activity at the tip was 0.0754 mmol l^{-1} s^{-1}, which is almost the same as that calculated without PGK activity. However, the ATPase activity at the tip of the flagellum increased up to 0.0895, 0.104 and 0.131 mmol l^{-1} s^{-1} when the concentration of the PGK substrates increased to 1.55, 3.1 and 6.2 mmol l^{-1}, respectively (Fig. 5C). These results indicate that PGK has a capacity to transfer high energy phosphoryls through spatial buffering of ATP when sufficient glycolytic intermediates are available.

Table 2. Parameters used for computations of Pi transport in flagella

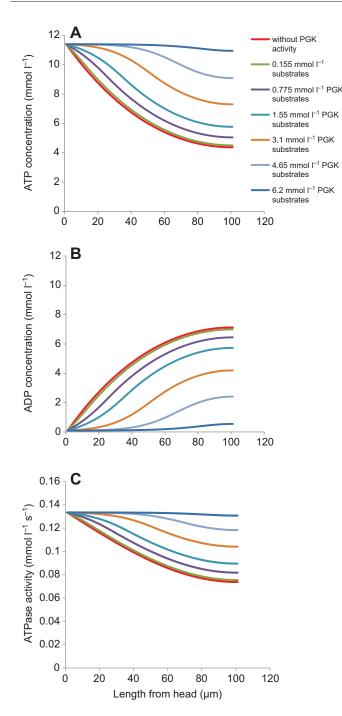| Parameters	Value	Reference
Flagellar length	100 µm	See Results
Diffusion coefficient for ANP	60 µm^2 s^{-1}	Takao and Kamimura, 2008
Diffusion coefficient for 3PG and 1,3BPG	104 µm^2 s^{-1}	Takao and Kamimura, 2008
PGK substrates concentration (total 3PG and 1,3BPG)	0.155 mmol l^{-1}	Determined by metabolomic analysis
Total adenine nucleotide	11.6 mmol l^{-1}	Determined by metabolomic analysis
Q_{1F}	0.134 mmol l^{-1} s^{-1}	Odet et al., 2011
K_I (K_m of ATPase from ATP, from ATP concentration for half-maximal beat frequency of demembranated flagella)	0.14 mmol l^{-1}	S. Ishijima (Tokyo Institute of Technology), personal data
K_i (for inhibition of flagellar beat frequency by ADP)	0.28 mmol l^{-1}	Okuno and Brokaw, 1979
K_{mP} (PGK2 K_m value for 3PG)	1.55 mmol l^{-1}	Pegoraro and Lee, 1978; Krietsch and Bücher, 1970
K_{mT} (PGK2 K_m value for ATP)	0.32 mmol l^{-1}	Pegoraro and Lee, 1978; Krietsch and Bücher, 1970
K_{mB} (PGK2 K_m value for 1,3BPG)	0.0022 mmol l^{-1}	Pegoraro and Lee, 1978; Krietsch and Bücher, 1970
K_{mD} (PGK2 K_m value for ADP)	0.16 mmol l^{-1}	Pegoraro and Lee, 1978; Krietsch and Bücher, 1970
Q_{2R}/Q_{2F} (ratio of reverse to forward PGK2)	2.71	Pegoraro and Lee, 1978; Krietsch and Bücher, 1970
K_A (myokinase K_m value for ATP)	0.3 mmol l^{-1}	Noda, 1973
K_N (myokinase K_m value for ADP)	0.3 mmol l^{-1}	Noda, 1973
K_M (myokinase K_m value for AMP)	0.3 mmol l^{-1}	Noda, 1973
Q_{3R}/Q_{3F} (ratio of reverse to forward adenylate kinase)	1.0	Noda, 1973
Cytosolic volume	53.5 fl	Yeung et al., 2002

K_m, Michaelis constant.

Fig. 5. Simulation of high energy phosphoryls diffusion along the flagellum. Calculated concentration profiles of ATP (A) and ADP (B), and calculated profiles of ATPase activity (C) without adenylate kinase activity using the parameters given in Table 2 and the equation indicated by Tombes et al. (Tombes et al., 1987).

DISCUSSION

Mammalian sperm must metabolize extracellular energy substrates to produce ATP for a long period to accomplish fertilization. Recently, many investigators reported about the relationship between metabolic pathway and flagellar motility in mouse sperm (Mukai and Okuno, 2004; Miki et al., 2004; Ford, 2006; Tanaka et al., 2004), but none of them focused on the different contributions of metabolic pathways to the flagellar movement. In the present study, we performed detailed analysis of mouse sperm flagellar

movement using various parameters to estimate the difference in contribution of metabolic pathways to mouse sperm motility, and revealed that glycolysis has an important role in energy transfer in mouse sperm flagella.

As reported previously (Mukai and Okuno, 2004; Miki et al., 2004; Tanaka et al., 2004), mouse sperm maintained vigorous motility for more than 60 min in the presence of energy substrates (glucose, pyruvate, BHB). There was no difference in motility parameters (beat frequency, bend angle, percentage of motility and sliding velocity) by substrates (Table 1). Because glucose is metabolized by glycolysis alone when sufficient glucose is available (Odet et al., 2011), these results indicate that mouse sperm are able to produce and supply an amount of ATP sufficient for maintaining motility by both glycolysis and respiration.

In contrast, ACH, which inhibits GAPDH through oxidation in cytoplasm (Mohri et al., 1975; Brown-Woodman et al., 1978; Stevenson and Jones, 1985), caused a significant decrease in the bend angle and sliding velocity even in the presence of respiratory substrates such as pyruvate or BHB (Fig. 1). Furthermore, measurements of local bending revealed flagellar bending was severely inhibited by ACH and DOG especially at the distal region of flagellum (Figs 2, 3). These results are inconsistent with a previous study (Tanaka et al., 2004). Detailed analysis of flagellar movement of the present study allowed us to evaluate motility change, which had been overlooked in the assessments of the percentage of motile sperm in the study of Tanaka et al. (Tanaka et al., 2004).

If the beat frequency is assumed to be constant throughout the flagellum as Okuno and Hiramoto (Okuno and Hiramoto, 1976) suggested, a decrease in local bending at the distal part of the flagellum indicates a decrease in sliding velocity of the doublet microtubule at that locus. Because the sliding velocity correlates with ATP concentration, the decreased bending suggests a decrease in ATP concentration at the distal part of the flagellum in glycolysis-inhibited sperm. By contrast, it is likely that the ATP level at the basal region of glycolysis-inhibited sperm is unchanged or almost saturated as beat frequency and local bending of the basal region were unaffected by ACH. This motility character resembles sea urchin sperm flagella in which the activity of creatine kinase is inhibited. In this case, creatine phosphate and creatine kinase are indispensable for energy supply from mitochondria located at the basal region of the flagellum to the distal end (Tombes et al., 1987; Tombes and Shapiro, 1985). Moreover, Shingyoji and colleagues (Shingyoji et al., 1995) reported about the relationship among ATP concentration, beat frequency, bend angle and sliding velocity using a head vibrating technique in demembranated sea urchin sperm as follows. The heads of demembranated sea urchin sperm, suspended in a certain concentration of ATP, were held by suction at the tip of a micropipette and vibrated laterally with respect to the head axis. When sperm were vibrated at frequencies higher than the undriven beat frequency of flagella, the apparent time-averaged sliding velocity of axonemal microtubules remained constant, with a higher frequency being accompanied by a decrease in the bend angle (Shingyoji et al., 1995). This phenomenon corresponds with the present study: the proximal region of the flagellum is assumed to contain a high concentration of ATP in the presence of respiratory substrates because mitochondria are located at the proximal region of the flagellum (mid piece), resulting in high sliding velocity therein. Generated bends propagate with a constant beat frequency to the distal end of the flagellum. However, a decrease in ATP concentration at the distal end of the flagellum by glycolysis inhibition causes a decrease in sliding velocity at the distal end, as

a consequence of the decrease in bend angle. Taken together, glycolysis inhibition by ACH (or DOG) probably induced a decrease in ATP, especially at the distal part of the flagellum even in the presence of respiratory substrates.

However, sperm swimming in the medium supplied with respiration substrates without glycolysis inhibition showed local bending and sliding velocity comparable to those observed in sperm supplied with glucose throughout the flagellum. This result suggests that sufficient ATP was supplied to the distal end of the flagellum. Taken together, it is likely that glycolysis has an important role in the supply of ATP to the distal end of the flagellum.

Because the decrease in ATP concentration at the distal part of flagellum is assumed to result in the decrease in total ATP in the sperm, total ATP in sperm was measured directly by reversed-phase HPLC. As shown in Fig. 4, the total ATP content was apparently reduced by ACH in pyruvate- and BHB-supplied sperm. By contrast, the ADP and AMP content was increased after ACH treatment. Because several mmol l^{-1} of ADP inhibits dynein ATPase in a competitive manner (Okuno and Brokaw, 1979), the increase in ADP, together with the decrease in ATP concentration, may impair microtubule sliding velocity. Therefore, it is likely that the reduction in sliding velocity by inhibition of glycolysis may be induced by both the decrease in ATP and increase in ADP.

It was previously proposed that ATP produced in mitochondria at the base of the flagellum is supplied to the distal part of the flagellum by simple diffusion (Nevo and Rikmenspoel, 1970). Tombes and colleagues, however, reported that sea urchin sperm could not maintain normal motility and failed in accomplishing fertilization without creatine kinase, an enzyme that catalyzes the reaction that is indispensable for the energy-transporting system (Tombes and Shapiro, 1985; Tombes et al., 1987). Because mouse sperm have three times longer flagella (120 μm) than sea urchin sperm (40 μm), it is predicted that ATP produced in mitochondria at the basal region of the flagellum cannot be supplied sufficiently by simple diffusion. Nevertheless, creatine kinase was not detected in mouse sperm (Kamp et al., 1996). Furthermore, knock-out of ubiquitous mitochondrial creatine kinase in mouse did not impact sperm motility and fertility (Steeghs et al., 1995). As mouse sperm apparently can supply adequate ATP from the base to the tip of the flagellum (Figs 2, 3), another energy supplying system in mouse sperm is predicted.

In skeletal muscle, an energy transferring system by glycolytic enzymes through ATP spatial buffering, called the near-equilibrium enzymatic flux network, was proposed recently (Dzeja et al., 2004; Dzeja and Terzic, 2003). In this system, individual glycolytic enzymes work as an ATP spatial buffer, replenishing ATP at the distal part of the flagellum. Sequential buffering reactions by glycolytic enzymes apparently 'transfer' a wave of high energy phosphoryls from basal mitochondria to the distal part of the flagellum. Based on their theory, we would like to propose a hypothesis about a new function of glycolysis as an energy transferring system in mouse sperm flagella. A schematic model of energy transfer by glycolytic enzymes is illustrated in Fig. 6. In this model, sequential rapid equilibrating reactions catalyzed by phosphoglycerate kinase (PGK) and GAPDH work in concert as a spatial ATP buffer, which transfers the 'energy wave' from the ATP producing site (mitochondria at the mid-piece) to ATP consuming sites (dynein arms along the flagellum) in the flagellum. To realize this ATP spatial buffer, it is essential that enzymes involved in the reaction distribute throughout the flagellum. From this point of view, glycolytic enzymes are suitable for supplying ATP because glycolytic enzymes localize to the fibrous sheath as a complex,
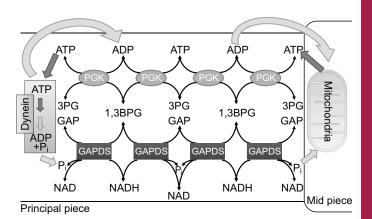

Fig. 6. Schematic model of energy transfer system by glycolysis. A schematic model of the energy transporting system in sperm flagella by glycolysis is illustrated by modifying the energy transfer system proposed by Dzeja and Terzic (Dzeja and Terzic, 2003) for sperm flagella. 1,3BPG, 1,3-bisphosphoglycerate; 3PG, 3-phosphoglycerate; GAP, glyceraldehyde-3-phosphate; GAPDS, glyceraldehyde-3-phosphate dehydrogenase, spermatogenic; NAD, nicotinamide adenine dinucleotide (oxidized); NADH, nicotinamide adenine dinucleotide (reduced); PGK, phosphoglycerate kinase; P_i, inorganic phosphate.

which runs along the entire length of the sperm tail. In addition, it is assumed that reduction in the flagellar bending at the distal part of the flagellum caused by ACH is attributed to the accumulation of inorganic phosphate (P_i), a product of ATP hydrolysis, because P_i acts as a competitive inhibitor, as demonstrated in demembranated sea urchin sperm motility, although the inhibition is not so strong (Okuno and Brokaw, 1979).

To validate the hypothesis that the glycolytic enzyme functions as an ATP spatial buffer, computer simulation of ANP diffusion along the flagellum was conducted based on the algorithms by Tombes et al. (Tombes et al., 1987). In this simulation, we adopted the reaction by PGK only because it is reported to be particularly important for transfer of high energy phosphoryls (Dzeja and Terzic, 2003). Although AK is abundantly present throughout the mouse sperm flagella (Cao et al., 2006), we ignored the reaction of AK because of the reasons described in the Results.

The ATPase activity at the distal end attenuated from 0.133 mmol l^{-1} s^{-1} (basal value) to 0.0738 mmol l^{-1} s^{-1} in the absence of the PGK reaction. Inclusion of the PGK activity did not significantly cause the recovery of ATPase activity at the tip of the flagellum (0.0754 mmol l^{-1} s^{-1}) when the concentration of PGK substrates (total 3PG and 1,3BPG) was 0.155 mmol l^{-1}, a value determined by metabolomic analysis (Table 2). Increase in the concentration of PGK substrates (~3.1 mmol l^{-1}), however, caused a recovery of ATPase activity to 0.104 mmol l^{-1} s^{-1}. Finally, ATPase activity at the tip did not decrease in the presence of PGK substrates as high as 6.2 mmol l^{-1} (0.131 mmol l^{-1} s^{-1}; Fig. 5). These results suggest that the PGK reaction potentially acts as an ATP spatial buffer, transferring energy in mouse sperm flagella when sufficient PGK substrates are available. In *Lactococcus lactis*, more than 10 mmol l^{-1} of 3PG was observed by ^{13}C-NMR analysis (Neves et al., 2000). In addition, 3PG and 1,3BPG concentrations in mouse brain cells were calculated to be 18.4 and 20.8 mmol l^{-1}, respectively, by computer simulation analysis (Oláh et al., 2008). In contrast to these reports, PGK substrate concentration determined by metabolomic analysis in the present experiment was much lower, 0.155 mmol l^{-1} (Table 2). Because 3PG and 1,3BPG are highly unstable compounds, it could be speculated that they have been

degraded during sample preparation in the present experiment, resulting in underestimation of the concentration of PGK substrates. The actual concentrations of PGK substrates could be enough for energy transfer in mouse sperm.

The ratio of total intracellular ATP to total ADP in glycolysis-non-inhibited sperm determined by HPLC measurements in the present experiments represented 5:2–6:2 (Fig. 4). This ratio, 5:2, is obtained by simulation when the PGK concentration is 1.55 mmol l^{-1}. Therefore, the experimental data seem to support that the actual value of intracellular PGK substrate is approximately 1.55 mmol l^{-1}.

In contrast, fitting of the results of the computer simulation to the results of flagellar movement analysis suggested a different concentration of PGK substrates. The ATPase activity at the tip of the flagellum calculated from the PGK activity in the presence of 6.2 mmol l^{-1} PGK substrates was 0.131 mmol l^{-1} s^{-1}. By contrast, the ATPase activity at the tip of the flagellum without PGK activity was 0.0738 mmol l^{-1} s^{-1}; the ratio between the two ATPase values was 0.56. This ratio was similar to the ratio of local bending of glycolysis-inhibited sperm to that of control sperm at the tip of the flagellum, which was approximately 0.5 (see Figs 2, 3). Changes in local bending along the flagellum in the presence of ACH obtained in the present experiments (Fig. 2C,D) and the simulated ATPase activity (Fig. 5C) are superimposed in Fig. 7. The relatively good coincidence between the two suggests that the energy transporting system by means of glycolysis could be employed in the flagellum. These results suggest that the realistic intracellular concentration of PGK substrates is approximately 6.2 mmol l^{-1}. Taken together, the concentration of PGK substrates was assumed to be 1.5–6.2 mmol l^{-1}. Under the present experimental conditions, such concentrations of PGK substrates might be realized by high concentrations of respiratory substrates, which would stop glycolytic flux; alternatively, high concentrations of respiratory substrates would replenish PGK substrates by reverse reactions that are conventionally considered irreversible under physiological conditions. Although the results from the computer simulation analysis strongly suggest that PGK has the potential to function as an ATP spatial buffer, transferring energy in mouse sperm flagella, further studies to determine the accurate value of PGK substrates concentration are necessary.

In conclusion, it was suggested that the ATP content in the distal part of flagellum is reduced by glycolysis inhibition even in the presence of the substrates of respiration. Based on this result, we proposed a new energy transfer system based on spatial buffering of
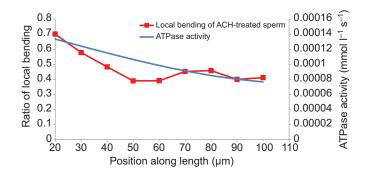

Fig. 7. Schematic model of the energy transporting system without glycolysis superimposed on the flagellar local bending inhibited by ACH. Simulated ATPase activity along flagellar axis in the absence of energy transporting system by glycolysis (Fig. 6C) is superimposed on the relative change in flagellar local bending when glycolysis is inhibited by ACH. Results from BHB + ACH (Fig. 3C) and pyruvate + ACH (Fig. 3D) are averaged.

ATP by glycolytic enzymes in mouse sperm. Further investigations about this new function of glycolysis in mouse sperm are needed, and would shed light on energy homeostasis not only in mammalian sperm physiology, but also in diverse motile cilia and flagella.

MATERIALS AND METHODS
Sperm preparation
Sperm were obtained from the cauda epididymis of 8- to 15-week-old ICR male mice (*Mus musculus* Linnaeus 1758) in accordance with the guidance of the University of Tokyo. The cauda epididymis was excised and punched with needles. Epididymal sperm was gently squeezed out and diluted into 100 µl of sucrose solution (300 mmol l^{-1} sucrose, 10 mmol l^{-1} Hepes-NaOH, pH 7.4), in which sperm exhibited very low activity (~1 Hz beat frequency), referred to as the initiated sperm by Fujinoki et al. (Fujinoki et al., 2001). The sperm suspension was diluted with the test solution for the analysis of sperm motility. The test solution contained 150 mmol l^{-1} NaCl, 5.5 mmol l^{-1} KCl, 0.4 mmol l^{-1} MgSO$_4$, 1 mmol l^{-1} CaCl$_2$, 10 mmol l^{-1} NaHCO$_3$, 10 mmol l^{-1} Hepes-NaOH (pH 7.4) and 10 mmol l^{-1} of metabolic substrates, such as glucose (Glc), pyruvate (Pyr) and BHB. One volume of sperm suspension was diluted into 20 volumes of each test solution and was incubated in a CO$_2$ incubator (37°C, 5% CO$_2$) for observation.

For the inhibition of glycolysis, either 10 mmol l^{-1} of ACH or 10 mmol l^{-1} of DOG was added to each test solution.

Analysis of sperm motility
After the incubation in the test solution containing metabolic substrates and inhibitors, an aliquot of sperm suspension was placed onto a prewarmed glass slide at 37°C and covered with a coverslip for observation with a microscope.

For the analysis of microtubule sliding velocity, sperm with their head attach to the glass surface were observed using a phase-contrast microscope (Diaphoto, Nikon, Tokyo, Japan), captured by a CCD camera (CR-20, Video Device, Chiba, Japan) and recorded by a video recorder (HR-G11, Victor JVC, Kanagawa, Japan). To analyze the sliding velocity, the flagellar waveforms were carefully traced by hand from a video monitor onto a transparent plastic film. The beat frequency was calculated from the number of video fields required to complete one beat cycle determined using the traced waveform. The bend angle of a flagellum was determined by measuring the angle between the tangents at two adjacent points of inflection when flagellar bends reach the center of the flagellum (Fig. 8A). Bend angle was measured for both principal bends (Fig. 8A, a) and reverse bends (Fig. 8A, b), and data were expressed as a sum of both values. Microtubule sliding velocity was calculated as the product of beat frequency and bend angle.
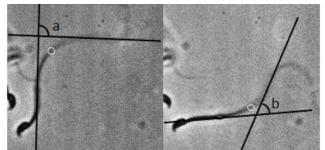
For the measurement of shear angle, sperm with their head attached to the glass surface were recorded digitally using a phase-contrast microscope and a computer-driven high-speed camera (HAS-220CH, DITECT, Tokyo, Japan). The shear angle of sperm flagella was analyzed by Bohboh, a flagellar movement auto-analyzing software kindly provided by Dr Shoji Baba (emeritus professor at Ochanomizu University, Tokyo, Japan). Shear angle was defined as the angle between the reference line at the base of the flagellum, usually parallel to the head axis, and the tangent at a point along the flagellum (see Fig. 8B). In the present experiment, shear angle was determined every 10 µm on the flagellum from the base to the tip for three cycles of beating. Then, difference between the maximum and minimum values was defined as a local amount of microtubule sliding per one beat cycle (Fig. 8B).

A local bend angle, defined as the angle between the tangents at the two inflection points around each vertex of the waveform, was determined on the images captured digitally by the high-speed camera. The analysis was conducted manually as the determination of bend angle. The distance of the bending vertex from the base of the flagellum was determined digitally using Bohboh software (Bohboh soft; Tokyo, Japan).
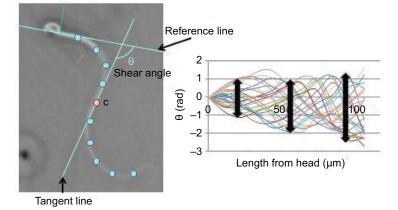
Measurement of ATP content by reversed phase HPLC
Evaluation of ATP content in mouse sperm cells was performed by reversed-phase HPLC (LC10VP series, Shimadzu, Kyoto, Japan) with slight

A Bend angle

B Shear angle

Fig. 8. Methods for the analysis of flagellar movement. (A) Analysis of bend angle. The bend angle of a flagellum was determined as follows. The angle between the tangents at two adjacent inflection points when flagellar bends reach the center of the flagellum (white circle) was measured. The angle was measured for both principal bends (a) and reverse bends (b), and bend angle is defined as the sum of both values. The bend angle was measured three times individually, and the bend angle of each spermatozoon was determined as their mean. (B) Analysis of shear angle. Shear angle at point c in the left picture was defined as the angle between the reference line at the base of the flagellum, usually parallel to the head axis, and the tangent at a point c. In the present experiment, shear angle was determined every 10 µm on the flagellum from the base to the tip for three cycles of beating (plotted in the right graph). Then, the difference between the maximum and minimum values (arrows in right graph) was defined as the local amount of microtubule sliding.

modifications (Mukai and Okuno, 2004; Samizo et al., 2001). Sperm suspended with each test solution in microtubes were incubated in a CO_2 incubator (5% CO_2, 37°C) for 30 min. One-tenth volume of 3% ice chilled perchloric acid was added to each sperm suspension to remove proteins, and the microtubes were placed on ice for 10 min. After centrifugation (10,000 *g*, 10 min, 4°C), the supernatant was filtered with a membrane of 0.22 µm pore size. The filtered solution was neutralized with phosphate buffer, and 25 µl of the neutralized solution was applied to a reversed-phase HPLC column (Phenomenex Luna 5 µC18, 4.6×150 mm; Shimadzu GLC, Tokyo, Japan). The mobile phase contained 20 mmol l^{-1} potassium phosphate (pH 6.8), 5 mmol l^{-1} tetrabutyl-ammonium hydroxide and 20% methanol. The number of sperm cells was counted in each sample, and the content of ATP was represented as nmol 10^{-6} sperm.

Metabolomic analysis
To determine the content of glycolytic intermediates, metabolome analysis was performed using the CE-TOFMS method. One milliliter of sperm suspension in sucrose solution was diluted into 10-fold volumes of each test solution containing 1 mmol l^{-1} glucose or 10 mmol l^{-1} pyruvate with or without 10 mmol l^{-1} ACH, and incubated for 30 min at 37°C. After incubation, 75% Percoll was added to the bottom of the tube and centrifuged for 5 min at 900 *g*, 4°C. Sperm were observed in the layer between the test solution and Percoll. The supernatant test solution was then discarded and the resultant was washed with 5% (w/w) mannitol solution to remove electrolytes. After centrifugation (900 *g*, 4°C, 2.5 min), supernatant was discarded and 1 ml of ice-cold methanol was added to fix sperm. Methanol-fixed sperm samples were separated by capillary electrophoresis and the amount of each intermediates was quantified by mass spectrometry. CE-TOFMS analysis was performed by Human Metabolome Technologies Inc. (Yamagata, Japan).

Computer simulation analysis of diffusion of ATP and high energy phosphoryls
Calculation of high energy phosphoryls diffusion along the flagellum was performed based on the algorithms previously reported by Tombes et al.

(Tombes et al., 1987). In the model, each molecular species diffusing along the flagellum is governed by a diffusion equation:

$$\frac{\partial C_{s,t}}{\partial t} = D \cdot \frac{\partial^2 C_{s,t}}{\partial s^2} + Q_{(s,t)} \,, \tag{1}$$

where $C_{s,t}$ represents the concentration of the diffusing species at position s and time t, D is the relevant diffusion coefficient, and Q is the rate of production of the species by chemical reactions. Q consisted of three reactions, specified by Q_1, Q_2 and Q_3, which are described below.

Q_1 is the dynein ATPase rate. Because the use of ATP by flagella is tightly coupled to motility, the relationship between the ATPase rate and the ATP concentration is assumed to be similar to the relationship between flagellar beat frequency and ATP concentration:

$$Q_1 = Q_{1F} \Bigg/ \left(1 + K_1 \left(1 + \frac{[ADP]}{K_i} \Big/ [ATP] \right) \right), \tag{2}$$

where K_1 is the ATP concentration for half-maximal beat frequency, and K_i is the constant for competitive inhibition of ATPase rate (beat frequency) by ADP. The maximum rate, Q_{1F}, with a value of 0.134 mmol l^{-1} s^{-1}, is based on measurements of glucose consumption by mouse sperm with the assumption that glucose is metabolized only by glycolysis (Odet et al., 2011). The K_1 value of 0.14 mmol l^{-1}, obtained from the measurements on demembranated ram sperm, was kindly provided by Dr Sumio Ishijima (Tokyo Institute of Technology). A value of 0.28 mmol l^{-1} was used for K_i, based on the measurements indicating that the value of K_i for demembranated sea urchin sperm flagella was twice the value of K_1 (Okuno and Brokaw, 1979). The reverse reaction for the ATPase is neglected.

Q_2 is the rate for the glycolytic reactions. Because the enzyme that catalyzes the first step of the ATP producing reaction (PGK) is reported to be particularly important for transferring high energy phosphoryls (Dzeja et al., 2004), only the reaction by PGK is included. This may be a good assumption, as glycolytic enzymes exist in a complex manner in spermatozoa (Westhoff and Kamp, 1997). The reaction by PGK is as follows:

$$ATP + 3PG \rightarrow ADP + 1,3BPG \,, \tag{3}$$

RESEARCH ARTICLE

The Journal of Experimental Biology (2014) doi:10.1242/jeb.090985

where 3PG represents 3-phosphoglycerate and 1,3BPG represents 1,3-bisphosphoglycerate. For this reaction, both forward and reverse rates are considered:

$$Q_2 = \frac{\left(Q_{2F} \frac{[3PG][ATP]}{K_{mP}K_{mT}} - Q_{2R} \frac{[1,3BPG][ADP]}{K_{mB}K_{mD}} \right)}{\left(1 + \frac{[3PG][ATP]}{K_{mP}K_{mT}} + \frac{[1,3BPG][ADP]}{K_{mB}K_{mD}} + \frac{[ATP]}{K_{mT}} + \frac{[3PG]}{K_{mP}} + \frac{[1,3BPG]}{K_{mB}} + \frac{[ADP]}{K_{mD}} \right)} . \quad (4)$$

Values used for the parameters in this equation are given in Table 2.

Q_3 is the rate for the adenylate kinase (Noda, 1973):

$$ATP + AMP \rightarrow 2ADP . \quad (5)$$

For this reaction also, both forward and reverse rates are considered:

$$Q_3 = \frac{\left(Q_{3F} \frac{[ATP][AMP]}{K_N K_M} - Q_{3R} \frac{[ADP][AMP]}{K_A K_A} \right)}{\left(1 + \frac{[ATP][AMP]}{K_N K_M} + \frac{[ADP][ADP]}{K_A K_A} + \frac{[ATP]}{K_N} + \frac{[AMP]}{K_M} + \frac{2[ADP]}{K_A} \right)} . \quad (6)$$

The parameters used to calculate this equation (Q_{3F}, Q_{3R}, K_N, K_M and K_A), which are originated from rabbit muscle fiber, are given in Table 2.

For each species, Q is the sum of the relevant rates as follows: for ATP, $Q=-Q_1-Q_2-Q_3$; for ADP, $Q=Q_1+Q_2+2Q_3$; for AMP, $Q=-Q_3$; for 3PG, $Q=-Q_2$; and for 1,3BPG, $Q=Q_2$.

If the diffusion coefficients for ATP, ADP and AMP and those for 3PG and 1,3BPG are assumed to be almost equivalent, there will be no gradient of total adenine nucleotide or total 3PG concentration along the flagellum. Thus, AMP can be obtained from (total adenine nucleotide – ATP – ADP) and 3PG can be obtained from (3PG + 1,3BPG) – 1,3BPG.

To solve the system of partial differential equations, three equations were integrated forward with time until a steady equilibrium solution was obtained. Concentrations at the basal end of the flagellum were held constant, and no fluxes were allowed past the distal end of the flagellum. Then, for each species, Eqn 1 was converted to:

$$C_{s,t+\Delta t} = C_{s,t} + D \left[\frac{(C_{s-\Delta s,t} - 2C_{s,t} + C_{s+\Delta s,t})}{\Delta s^2} \right] \Delta t + Q_{s,t} \cdot \Delta t . \quad (7)$$

The length interval, Δs, was 1 μm in all the results shown, and the time interval, Δt, was normally 0.5 ms. The simulation program was written in and performed using the computer software Mathematica (Wolfram Research, Champaign, IL, USA).

Statistical analysis

Values for sliding velocity, shear angle and ATP content were expressed as means ± s.e.m. Statistical tests were performed using Student's t-test to test for differences in the content of adenine nucleotides. In the other experiments, data were analyzed by ANOVA and *post hoc* Tukey–Kramer tests.

Reagents

ACH was purchased from Sigma-Aldrich (St Louis, MO, USA), BHB was from MP Biomedicals (Santa Ana, CA, USA), Percoll was from GE Healthcare (Chalfont St Giles, UK), and the other chemicals were purchased from Wako Pure Chemicals Co. Ltd (Osaka, Japan).

Acknowledgements
We are grateful to Dr Shoji A. Baba of Ochanomizu University for providing the flagellar movement auto-analyzing software Bohboh. We thank Dr Sumio Ishijima of the Tokyo Institute of Technology for providing us the K_1 value of demembranated ram sperm.

Competing interests
The authors declare no competing financial interests.

Author contributions
G.L.T. contributed to the design and execution of all the experiments. D.M. contributed to the execution of the computer simulation experiment. C.M. contributed to the design of the biochemical experiments. M.O. contributed to the conception and general design of all the experiments. This work was developed from previous work (Mukai and Okuno, 2004).

Funding
Part of this research was supported by a Sasakawa Scientific Research Grant [22-454 to G.L.T.], and by Japan Society for the Promotion of Science Grants-in-Aid for Scientific Research [Wakate B to C.M. and 17049012 to M.O.].

References

Austin, C. R. (1985). Sperm maturation in the male and female genital tracts. In *Biology of Fertilization: Biology of the Sperm*, Vol. 2 (ed. C. B. Metz and A. Monroy), pp. 121-155. New York, NY: Academic Press.

Brown-Woodman, P. D. C., Mohri, H., Mohri, T., Suter, D. and White, I. G. (1978). Mode of action of α-chlorohdrin as a male anti-fertility agent. Inhibition of the metabolism of ram spermatozoa by alpha-chlorohydrin and location of block in glycolysis. *Biochem. J.* **170**, 23-37.

Cao, W., Haig-Ladewig, L., Gerton, G. L. and Moss, S. B. (2006). Adenylate kinases 1 and 2 are part of the accessory structures in the mouse sperm flagellum. *Biol. Reprod.* **75**, 492-500.

Danshina, P. V., Geyer, C. B., Dai, Q., Goulding, E. H., Willis, W. D., Kitto, G. B., McCarrey, J. R., Eddy, E. M. and O'Brien, D. A. (2010). Phosphoglycerate kinase 2 (PGK2) is essential for sperm function and male fertility in mice. *Biol. Reprod.* **82**, 136-145.

Dzeja, P. P. and Terzic, A. (2003). Phosphotransfer networks and cellular energetics. *J. Exp. Biol.* **206**, 2039-2047.

Dzeja, P. P., Terzic, A. and Wieringa, B. (2004). Phosphotransfer dynamics in skeletal muscle from creatine kinase gene-deleted mice. *Mol. Cell. Biochem.* **256-257**, 13-27.

Ford, W. C. L. (2006). Glycolysis and sperm motility: does a spoonful of sugar help the flagellum go round? *Hum. Reprod. Update* **12**, 269-274.

Ford, W. C. L. and Harrison, A. (1985). The presence of glucose increases the lethal effect of alpha-chlorohydrin on ram and boar spermatozoa *in vitro*. *J. Reprod. Fertil.* **73**, 197-206.

Ford, W. C. L. and Harrison, A. (1986). The concerted effect of alpha-chlorohydrin and glucose on the ATP concentration in spermatozoa is associated with the accumulation of glycolytic intermediates. *J. Reprod. Fertil.* **77**, 537-545.

Fujinoki, M., Ohtake, H. and Okuno, M. (2001). Serine phosphorylation of flagellar proteins associated with the motility activation of hamster spermatozoa. *Biomed. Res.* **22**, 45-58.

Hiipakka, R. A. and Hammerstedt, R. H. (1978). 2-Deoxyglucose transport and phosphorylation by bovine sperm. *Biol. Reprod.* **19**, 368-379.

Hyne, R. V. and Edwards, K. P. (1985). Influence of 2-deoxy-D-glucose and energy substrates on guinea-pig sperm capacitation and acrosome reaction. *J. Reprod. Fertil.* **73**, 59-69.

Kamp, G., Büsselmann, G. and Lauterwein, J. (1996). Spermatozoa: models for studying regulatory aspects of energy metabolism. *Experientia* **52**, 487-494.

Krietsch, W. K. and Bücher, T. (1970). 3-phosphoglycerate kinase from rabbit scletal muscle and yeast. *Eur. J. Biochem.* **17**, 568-580.

Krisfalusi, M., Miki, K., Magyar, P. L. and O'Brien, D. A. (2006). Multiple glycolytic enzymes are tightly bound to the fibrous sheath of mouse spermatozoa. *Biol. Reprod.* **75**, 270-278.

Miki, K., Qu, W., Goulding, E. H., Willis, W. D., Bunch, D. O., Strader, L. F., Perreault, S. D., Eddy, E. M. and O'Brien, D. A. (2004). Glyceraldehyde 3-phosphate dehydrogenase-S, a sperm-specific glycolytic enzyme, is required for sperm motility and male fertility. *Proc. Natl. Acad. Sci. USA* **101**, 16501-16506.

Mohri, H., Suter, D. A. I., Brown-Woodman, P. D. C., White, I. G. and Ridley, D. D. (1975). Identification of the biochemical lesion produced by α-chlorohydrin in spermatozoa. *Nature* **255**, 75-77.

Mukai, C. and Okuno, M. (2004). Glycolysis plays a major role for adenosine triphosphate supplementation in mouse sperm flagellar movement. *Biol. Reprod.* **71**, 540-547.

Neves, A. R., Ramos, A., Shearman, C., Gasson, M. J., Almeida, J. S. and Santos, H. (2000). Metabolic characterization of *Lactococcus lactis* deficient in lactate dehydrogenase using *in vivo* ¹³C-NMR. *Eur. J. Biochem.* **267**, 3859-3868.

Nevo, A. C. and Rikmenspoel, R. (1970). Diffusion of ATP in sperm flagella. *J. Theor. Biol.* **26**, 11-18.

Noda, L. (1973). Adenylate kinase. In *The Enzymes,* Vol. VIII (ed. P. D. Boyer), pp. 279-305. New York, NY: Academic Press.

Odet, F., Duan, C., Willis, W. D., Goulding, E. H., Kung, A., Eddy, E. M. and Goldberg, E. (2008). Expression of the gene for mouse lactate dehydrogenase C (Ldhc) is required for male fertility. *Biol. Reprod.* **79**, 26-34.

Odet, F., Gabel, S. A., Williams, J., London, R. E., Goldberg, E. and Eddy, E. M. (2011). Lactate dehydrogenase C and energy metabolism in mouse sperm. *Biol. Reprod.* **85**, 556-564.

Okuno, M. and Brokaw, C. J. (1979). Inhibition of movement of trition-demembranated sea-urchin sperm flagella by Mg²⁺, ATP⁴⁻, ADP and P$_i$. *J. Cell Sci.* **38**, 105-123.

Okuno, M. and Hiramoto, Y. (1976). Mechanical stimulation of starfish sperm flagella. *J. Exp. Biol.* **65**, 401-413.

Oláh, J., Klivényi, P., Gardián, G., Vécsei, L., Orosz, F., Kovacs, G. G., Westerhoff, H. V. and Ovádi, J. (2008). Increased glucose metabolism and ATP level in brain tissue of Huntington's disease transgenic mice. *FEBS J.* **275**, 4740-4755.

Pegoraro, B. and Lee, C. Y. (1978). Purification and characterization of two isozymes of 3-phosphoglycerate kinase from the mouse. *Biochim. Biophys. Acta* **522**, 423-433.

Samizo, K., Ishikawa, R., Nakamura, A. and Kohama, K. (2001). A highly sensitive method for measurement of myosin ATPase activity by reversed-phase high-performance liquid chromatography. *Anal. Biochem.* **293**, 212-215.

The Journal of Experimental Biology

Shingyoji, C., Yoshimura, K., Eshel, D., Takahashi, K. and Gibbons, I. R. (1995). Effect of beat frequency on the velocity of microtubule sliding in reactivated sea urchin sperm flagella under imposed head vibration. *J. Exp. Biol.* **198**, 645-653.

Si, Y. and Okuno, M. (1995). Activation of mammalian sperm motility by regulation of microtubule sliding via cyclic adenosine 5′-monophosphate-dependent phosphorylation. *Biol. Reprod.* **53**, 1081-1087.

Steeghs, K., Oerlemans, F. and Wieringa, B. (1995). Mice deficient in ubiquitous mitochondrial creatine kinase are viable and fertile. *Biochim. Biophys. Acta* **1230**, 130-138.

Stevenson, D. and Jones, A. R. (1985). Production of (S)-3-chlorolactaldehyde from (S)-α-chlorohydrin by boar spermatozoa and the inhibition of glyceraldehyde 3-phosphate dehydrogenase *in vitro*. *J. Reprod. Fertil.* **74**, 157-165.

Takao, D. and Kamimura, S. (2008). FRAP analysis of molecular diffusion inside sea-urchin spermatozoa. *J. Exp. Biol.* **211**, 3594-3600.

Tanaka, H., Takahashi, T., Iguchi, N., Kitamura, K., Miyagawa, Y., Tsujimura, A., Matsumiya, K., Okuyama, A. and Nishimune, Y. (2004). Ketone bodies could support the motility but not the acrosome reaction of mouse sperm. *Int. J. Androl.* **27**, 172-177.

Tombes, R. M. and Shapiro, B. M. (1985). Metabolite channeling: a phosphorylcreatine shuttle to mediate high energy phosphate transport between sperm mitochondrion and tail. *Cell* **41**, 325-334.

Tombes, R. M., Brokaw, C. J. and Shapiro, B. M. (1987). Creatine kinase-dependent energy transport in sea urchin spermatozoa. Flagellar wave attenuation and theoretical analysis of high energy phosphate diffusion. *Biophys. J.* **52**, 75-86.

Welch, J. E., Brown, P. L., O'Brien, D. A., Magyar, P. L., Bunch, D. O., Mori, C. and Eddy, E. M. (2000). Human glyceraldehyde 3-phosphate dehydrogenase-2 gene is expressed specifically in spermatogenic cells. *J. Androl.* **21**, 328-338.

Westhoff, D. and Kamp, G. (1997). Glyceraldehyde 3-phosphate dehydrogenase is bound to the fibrous sheath of mammalian spermatozoa. *J. Cell Sci.* **110**, 1821-1829.

Yano, Y. and Miki-Noumura, T. (1980). Sliding velocity between outer doublet microtubules of sea-urchin sperm axonemes. *J. Cell Sci.* **44**, 169-186.

Yeung, C. H., Anapolski, M. and Cooper, T. G. (2002). Measurement of volume changes in mouse spermatozoa using an electronic sizing analyzer and a flow cytometer: validation and application to an infertile mouse model. *J. Androl.* **23**, 522-528.